Physica C 506 (2014) 69–75

Contents lists available at ScienceDirect

Physica C

journal homepage: www.elsevier.com/locate/physc

Dual role of an ac driving force and the underlying two distinct order–disorder transitions in the vortex phase diagram of $Ca_3Ir_4Sn_{13}$

Santosh Kumar [a,*], Ravi P. Singh [b,1], A. Thamizhavel [b], C.V. Tomy [a,2], A.K. Grover [b,c]

[a] Department of Physics, Indian Institute of Technology Bombay, Mumbai 400076, India
[b] Department of Condensed Matter Physics and Materials Science, Tata Institute of Fundamental Research, Mumbai 400005, India
[c] Department of Physics, Panjab University, Chandigarh 160014, India

ARTICLE INFO

Article history:
Received 20 May 2014
Received in revised form 2 July 2014
Accepted 27 August 2014
Available online 10 September 2014

Keywords:
Peak effect
Second magnetization peak
First-order transition

ABSTRACT

We present distinct demarcation of the Bragg glass (BG) to multi-domain vortex glass (VG) transition line and the eventual amorphization of the VG phase in a weakly pinned single crystal of the superconducting compound $Ca_3Ir_4Sn_{13}$ on the basis of comprehension of the different yields about the second magnetization peak (SMP) anomaly in the dc magnetization and the corresponding anomalous feature in the ac susceptibility measurements. The shaking by a small ac magnetic field, inevitably present in the ac susceptibility measurements, is seen to result in contrasting responses in two different portions of the field-temperature (H, T) phase space of the multi-domain VG. In one of the portions, embracing the BG to VG transition across the onset of the SMP anomaly, the ac drive is surprisingly seen to assist the transformation of the well ordered BG phase to a lesser ordered VG phase. The BG phase exists as a superheated state over a small portion of the VG space and this attests to the first order nature of the BG to VG transition.

1. Introduction

The advent of high T_c superconductivity [1] had made it enlightening and relevant to locate different phase boundaries in the H–T phase space [2–9], depicting the various possible phase transformations for the vortex matter in a type-II superconductor. A widely investigated anomaly elucidating the features of the vortex phase diagram of a high T_c cuprate superconductor, $YBa_2Cu_3O_7$ (YBCO) [9–16], has been the peak effect (PE) phenomenon [2], which amounts to a sudden increase in the otherwise monotonically decreasing critical current density (j_c) just before reaching the upper critical field line, $H_{c2}(T)$. As per the Larkin–Ovchinnikov [17] description, j_c is related inversely to the volume (V_c) ($j_c \propto 1/\sqrt{V_c}$) of the domain within which the displacements of the individual flux lines remain well correlated. Hence, an anomalous increase in $j_c(H,T)$ (as in PE phenomenon) signifies a shrinkage in V_c, which in turn, amounts to an order–disorder transformation of the vortex matter. Somewhat analogous to the PE, there is another anomalous feature occurring deep inside the mixed state (well below H_{c2}), called the second magnetization peak (SMP) [9,15,16,18–24] which also imprints as a non-monotonic behavior of $j_c(H)$. The SMP feature has been well studied in high T_c cuprate superconductors, $YBa_2Cu_3O_7$ (YBCO) [9], $Bi_2Sr_2CaCu_2O_8$ (BSCCO) [20,21] and another oxide superconductor, (Ba,K) BiO system[22–24].

As an important consequence of the above mentioned studies of the vortex phase transformations in the high T_c superconductors, the PE/SMP behavior and the vortex phase diagrams have been revisited various times in several conventional superconductors, such as, Nb [25–27], 2H-$NbSe_2$ [2,3,7,28–33], YNi_2B_2C [34,35], $LuNi_2B_2C$ [34] $Ca_3Rh_4Sn_{13}$ [16,36–39], $Yb_3Rh_4Sn_{13}$ [40,41], etc. The order–disorder transitions (*a la* PE and SMP) reported in $Ca_3Rh_4Sn_{13}$ (CaRhSn) by some of the present authors [16] bore a marked resemblance with characteristic results in some single crystals of the high T_c superconductor YBCO. In addition, a recent report [39] of an exemplification of the notion of inverse melting of the vortex lattice in a crystal of CaRhSn echoes well with the similar characteristic in the high T_c superconductors YBCO [42] and BSCCO [43]. The above mentioned investigations in the low T_c superconductors have thus lead to the revelation of many instructive aspects of the PE and the SMP anomalies. For example, the results of small angle neutron scattering (SANS) together with ac susceptibility measurements performed concurrently in a single

* Corresponding author.
E-mail addresses: santoshkumar@phy.iitb.ac.in (S. Kumar), tomy@phy.iitb.ac.in (C.V. Tomy).
[1] Present address: Department of Physics, Indian Institute of Science Education and Research, Bhopal 462066, India
[2] Principal corresponding author.

http://dx.doi.org/10.1016/j.physc.2014.08.009
0921-4534/

crystal of Nb provided convincing evidence of a quasi-first-order transition, from flux line lattice to amorphous vortex solid, across the onset of the PE anomaly [26]. The SMP on the other hand, is widely accepted [9,18,19] as a disorder or pinning-induced transition amounting to a well ordered Bragg glass (BG) state transforming to a *multi-domain* vortex glass (VG) phase [4,5,20,44]. The first-order nature of BG to VG transition, however, awaits convincing elucidation. In spite of advances in understanding and continuous updating of the vortex phase diagrams of a variety of type-II superconductors [32,33,35,45], several issues still remained to be fully comprehended. One of these is the delineation between the SMP and PE anomalies when they juxtapose, and the underlying physics represented by them.

Motivated by the aforesaid interesting features reported for a variety of superconductors, we have now investigated another low T_c (~ 7.10 K) [46–48] superconductor $Ca_3Ir_4Sn_{13}$, which belongs to the family of ternary stannides [49] having cubic structure. This compound has attracted particular attention in recent years. For example, there have been evidences for nodeless superconductivity [48] and a coexistence of superconductivity and ferromagnetic spin fluctuations [47] (attributed to Ir 4d-band) in $Ca_3Ir_4Sn_{13}$. However, to the best of our knowledge, studies related to vortex phase transformations in its superconducting mixed state have not been reported in this compound. In this work, we present a comparison of different outcomes of the ac and dc magnetization measurements performed in a weakly pinned (ratio of depinning and depairing current densities is $\sim 10^{-5}$) single crystal of $Ca_3Ir_4Sn_{13}$. The magnetization data reveal a very broad composite anomalous variation in $j_c(H,T)$ which amounts to an order–disorder transformation in the vortex matter, however, the specific phase boundaries, pertaining to the order–disorder transformation, obtained from the ac and the dc measurement techniques are found to be significantly different. We can identify a certain region of the phase space where the ac field unexpectedly assists the transformation of the quasi-ordered BG into the partially disordered VG phase. In a different region of the *H*–*T* phase space, the ac drive is seen to enhance the quality of spatial order of the underlying vortex matter, which inter alia is indicative of another order–disorder transition occurring in that portion of phase space, which gets exposed under the influence of an ac field. The two contrasting roles of the ac drive in different portions are attributed to the juxtaposition of the SMP anomaly (pinning induced) and the peak effect (PE) phenomenon (collapse of elasticity induced amorphization of the vortex matter). The unusual outcome of the imposition of an ac drive near the onset field of SMP anomaly in the present report also corroborates a very recent finding [50] in a different class of superconductor, (i.e., in $Ba_{0.5}K_{0.5}Fe_2As_2$), wherein a large ac field ($\sim$ 12 Oe) lowers the onset field value of the anomalous change in j_c at a given temperature, thereby elucidating the role of ac driving force in facilitating the spatial disordering of the vortex matter in a portion of the phase-space where the ordered state is metastable superheated state.

2. Experimental details

The single crystals of $Ca_3Ir_4Sn_{13}$ were grown by tin flux method [46]. The crystal chosen for the present study is platelet shaped, with a planar area of 4.7 mm^2 and with thickness of 0.64 mm, and mass of 26.2 mg. The ac and dc magnetization measurements were performed in a Superconducting Quantum Interference Device–Vibrating Sample Magnetometer (SQUID–VSM, Quantum Design Inc., USA). The amplitude of the vibration in SQUID-VSM was kept small for all the dc magnetization measurements so as to avoid artifact that could arise from possible magnetic field inhomogeneity of a superconducting magnet along the length of sample movement. The ac magnetization measurements were performed by superimposing an oscillating magnetic field on various dc magnetic fields. The peak amplitude and the frequency of the driving ac field were chosen as 3.5 Oe and 211 Hz, respectively.

3. Results

3.1. Ac susceptibility: identification of anomalous variation in critical current density

3.1.1. Isofield ac susceptibility measurements

Fig. 1(a) shows the temperature dependences of the real part of the isofield ac susceptibility ($\chi'(T)$) in dc fields (applied parallel to plane of the platelet shaped sample), as indicated. The $\chi'(T)$ plots have been normalized with respect to the saturated value of χ' recorded at $T = 2$ K for $H_{dc} = 0$. The $\chi'(T)$ curve for $H_{dc} = 0$ shows the saturated behavior at low temperatures (see the inset (i) of Fig. 1(a)), revealing the characteristic full magnetic shielding effect, typical of a superconductor. The superconducting transition temperature, $T_c(H_{dc} = 0) \approx 7.1$ K, obtained via the onset of diamagnetic response (see expanded plot in the inset (ii) of Fig. 1(a))

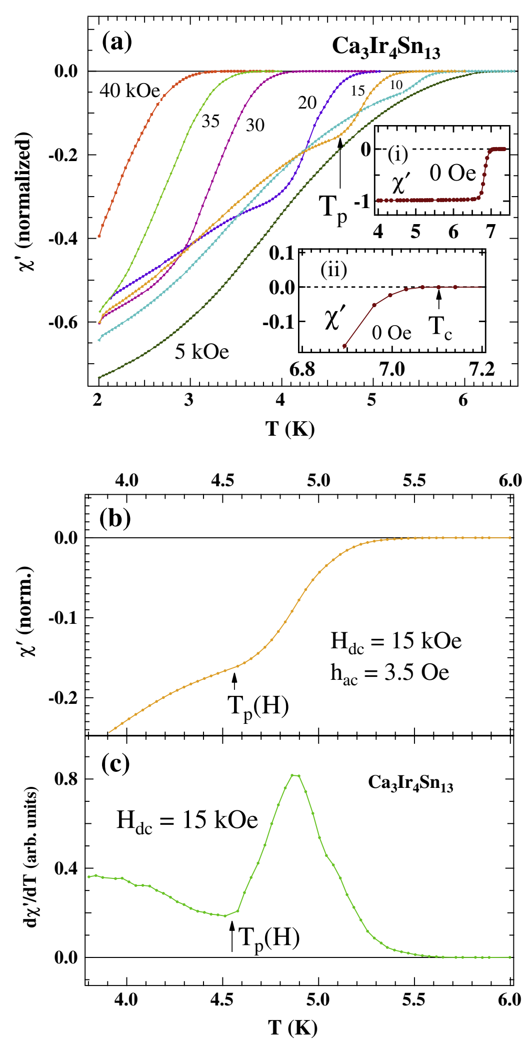

Fig. 1. (a) Real part of the ac susceptibility, $\chi'(T)$ (in normalized units) plotted against temperature at various dc magnetic fields (applied parallel to the plane of platelet shaped crystal and as indicated). Inset (i) shows the saturated $\chi'(T)$ response for $H_{dc} = 0$, and the inset (ii) displays its magnified portion near T_c. (b) Portion of $\chi'(T)$ curve for $H_{dc} = 15$ kOe showing an anomalous modulation prior to the transition to the normal state. (c) Portion of derivative plot of $\chi'(T)$ (with respect to *T*) for $H_{dc} = 15$ kOe locating the temperature ($T_p(H)$) corresponding to a position of a maximum in $j_c(T)$.